Supporting Information

Heterogeneous Structured $MoSe_2$-MoO_3 Quantum Dots with Enhanced Sodium/Potassium Storage

Wen Liu, [a, c] Jujun Yuan, [b*] Youchen Hao, [a, c] Hirbod Maleki Kheimeh Sari, [a, c] Jingjing wang, [a, c] Alibek Kakimov, [a, c] Wei Xiao, [a, c] Jian Qin, [a, c] Wenbin Li, [a, c] Chong Xie [a, c] Junhua Hu, [d] Jianhong Peng, [e*] Xifei Li [a, c*]

[a]Institute of Advanced Electrochemical Energy & School of Materials Science and Engineering, Xi'an University of Technology, Xi'an 710048, Shaanxi, China

[b]School of Physics and Electronics, Gannan Normal University, Ganzhou, 341000, PR China

[c]Shaanxi International Joint Research Center of Surface Technology for Energy Storage Materials, Xi'an 710048, Shaanxi, China

[d]State Center for International Cooperation on Designer Low-carbon & Environmental Materials (CDLCEM), Zhengzhou University, Zhengzhou, China

[e]School of Physical and Electronic Information Engineering, Qinghai Nationalities University, Xining, China

*Corresponding author. E-mail: xfli2011@hotmail.com, yuanjujun123@163.com, pjhhj@sohu.com

Electrochemical impedance spectroscopy (EIS) analysis

Each of the resulting impedance spectra comprises three regions: (i) a semicircle in high frequency region related to the solid electrolyte interphase (SEI); (ii) a semicircle in intermediate frequency region representing the charge interfacial capacitance and transfer resistance at the electrode/electrolyte interface; (iii) a sloping line in low frequency region associated with the Warburg impedance representing the Li-ion diffusion through the solid electrode. In the equivalent circuit as shown in Fig. S7, R_s represents the resistance of the electrolyte solution, R_f is the resistance of the surface SEI, R_{ct} corresponds to the charge transfer resistance, CPE is the capacitance of the electrode/electrolyte double layer, and Ws represents the Warburg impedance. All of the impedance spectra were fitted with the equivalent circuit to calculate the values of Rs, and R_{f+ct}, as listed in Table 1.

Meanwhile, the Na^+ diffusion is measured based on the analysis of impedance and according to Equations (1) and (2):

$$D_{Na+} = R^2 T^2 / 2 n^4 F^4 \sigma_w^2 A^2 C^2 \quad (1)$$

$$Z' = R + \sigma_w \omega^{-1/2} \quad (2)$$

EIS was employed to calculate the Na^+ transfer coefficient to study the effect of crystallinity on sodium storage performance. In Equations (1) and (2), R, T, n, F, A, C, and σ_w are the gas constant (8.314 J/(mol·K)), the absolute temperature (301.15 K), the number of electrons per molecule during oxidation (2), the Faraday's constant (96485 C mol^{-1}), the surface area of the electrode (1.13 cm^2), the Na^+ concentration in the electrode material (1.0 mol L^{-1}), and the Warburg coefficient, respectively.

Galvanostatic intermittent titration technique (GITT)

For the GITT measurements, the cells were charged at a current density of 0.05 A g^{-1} for 20 min, followed by an open circuit relaxation for 2 h.

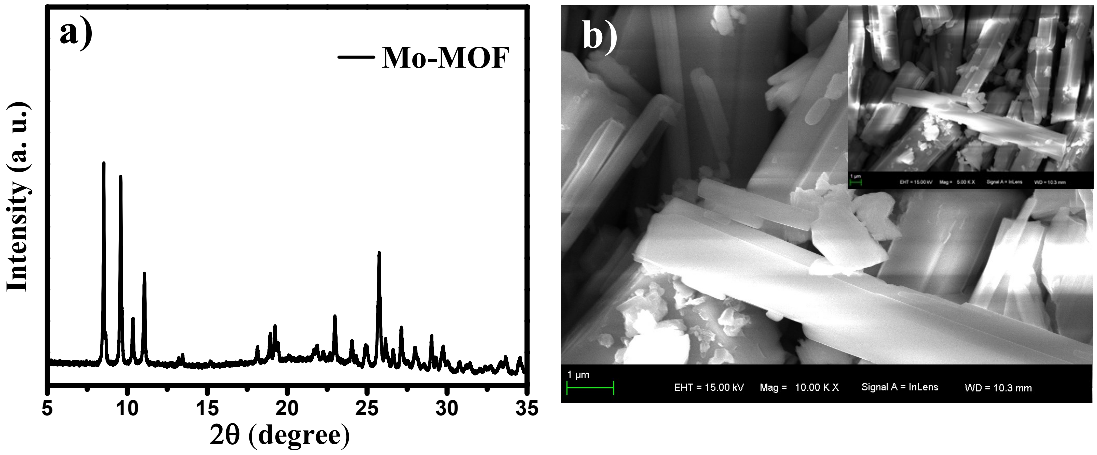

Fig. S1. a) XRD spectrum and b) SEM images of the synthesized molybdenum-based MOF (Mo-MOF).

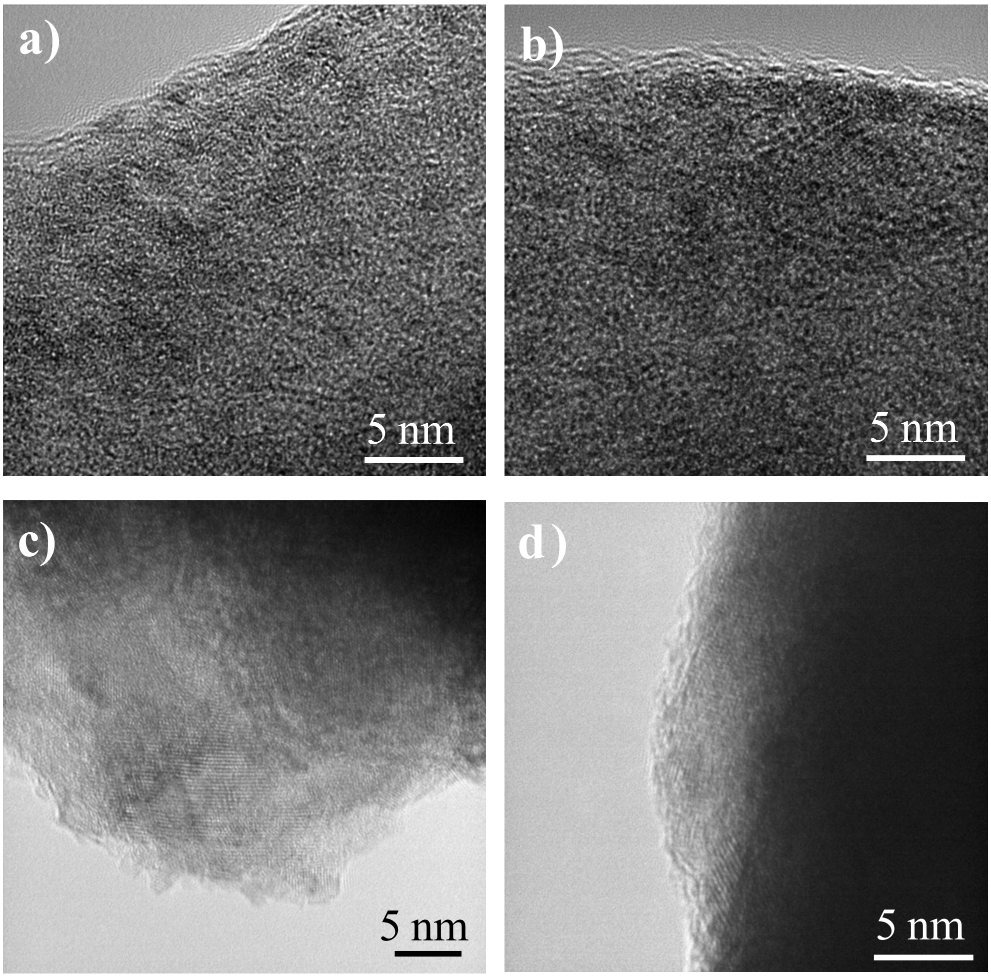

Fig. S2. HRTEM images of a, b) $MoSe_2$-1 and c, d) $MoSe_2$-4.

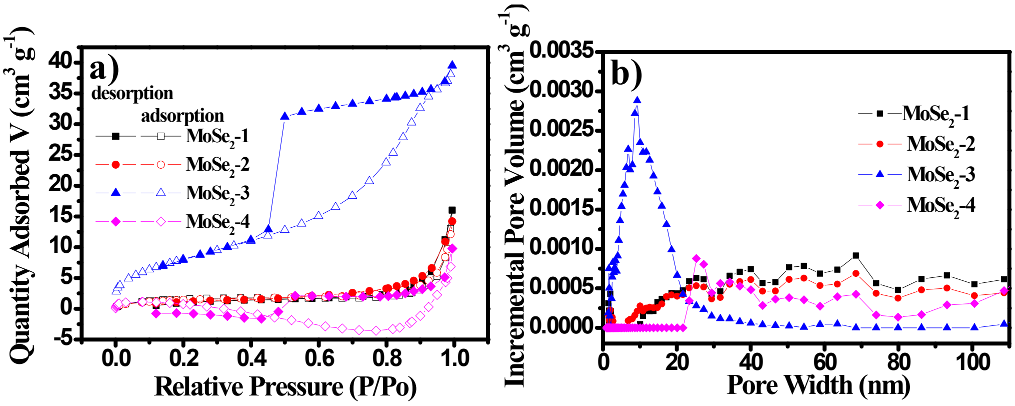

Fig. S3. a) Adsorption/desorption isotherms, b) The pore size distribution of $MoSe_2$-1, $MoSe_2$-2, $MoSe_2$-3, and $MoSe_2$-4.

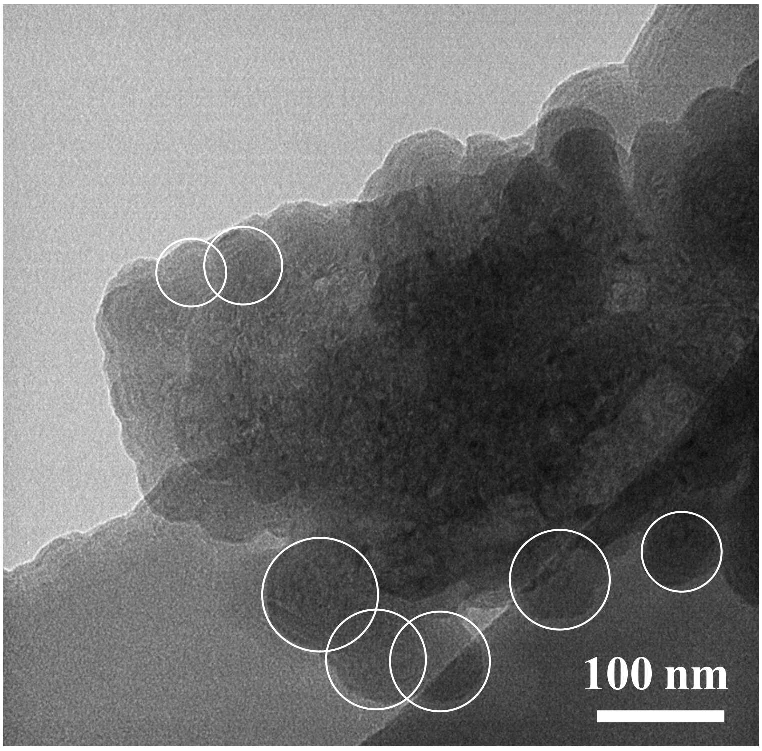

Fig. S4. TEM image of $MoSe_2$-3.

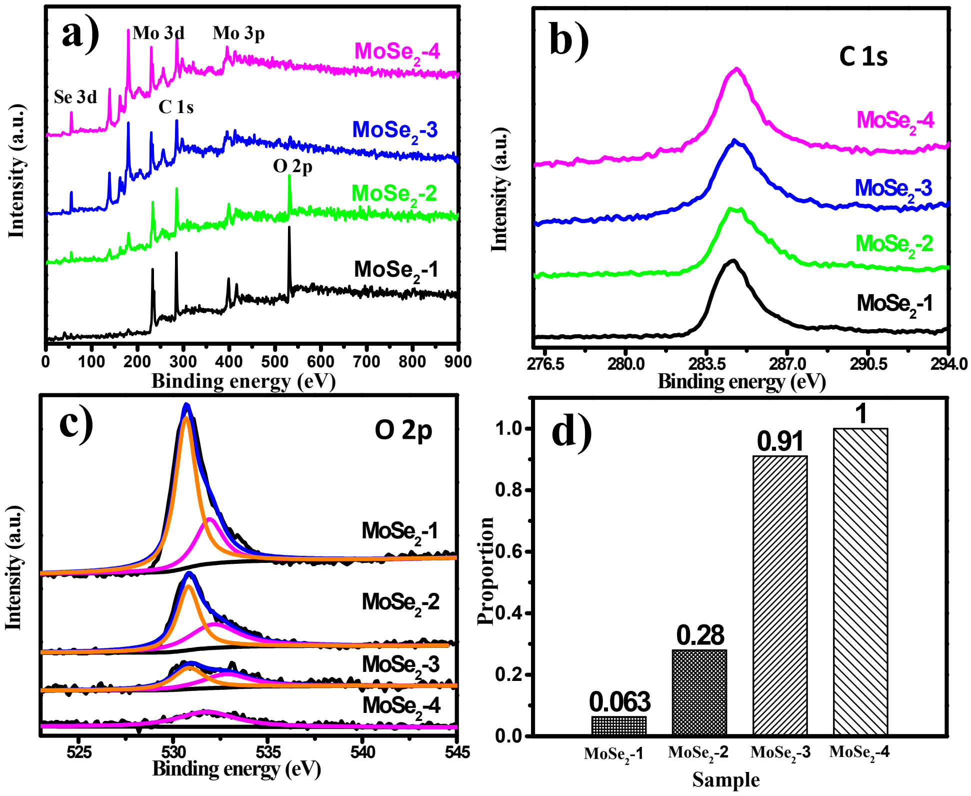

Fig. S5. XPS spectra of $MoSe_2$-1, $MoSe_2$-2, $MoSe_2$-3, and $MoSe_2$-4: a) The XPS full spectra for b) C 1s, and c) O 2p. d) The molar proportion of Mo from $MoSe_2$ in the total Mo content of samples.

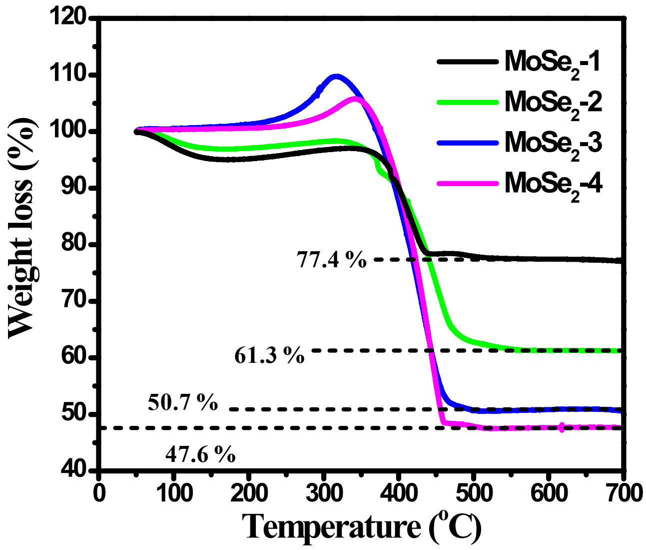

Fig. S6. TGA curves of $MoSe_2$-1, $MoSe_2$-2, $MoSe_2$-3, and $MoSe_2$-4.

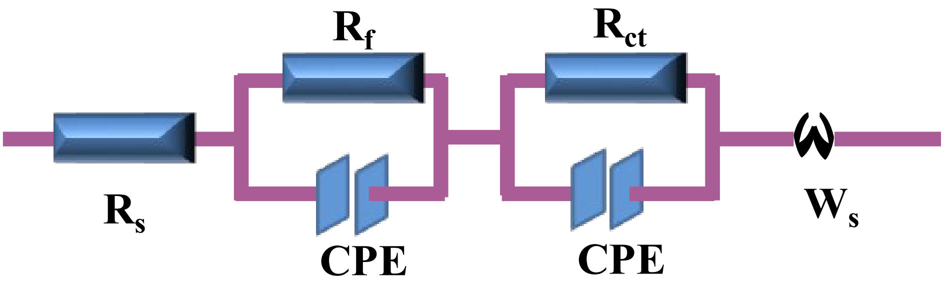

Fig. S7. The equivalent circuit for the fitting electrochemical impedance spectroscopy.

Table S1. The loading of MoO_3, $MoSe_2$ and C in the four samples.

samples	The percentage of MoO_3, $MoSe_2$ and C		
	MoO_3	$MoSe_2$	C
$MoSe_2$-1	72.53	8.6	18.87
$MoSe_2$-2	44.2	30.3	25.5
$MoSe_2$-3	4.54	80.92	14.54
$MoSe_2$-4	---	83.96	16.04

Table S2. The performance of optimized sample in this work in comparision with the previously reported $MoSe_2$ composites for SIBs.

Anode	Performance	Retention, Attenuation Per cycle	Ref.
MoSe2-MoO3/C	400 mAh/g after 500 cycles at 0.1 A/g	90%, 0.02%	This work
MoSe2/N,P-rGO	378 mAh/g after 1000 cycles at 0.5 A/g	87%, 0.013%	1
MoSe2/N-C	329 mAh/g after 500 cycles at 1.0 A/g	88.5%, 0.023%	2
CNT/MoSe2/C	347 mAh/g after 500 cycles at 0.5 A/g	93.5%, 0.013%	3
MoSe2/N-C	333 mAh/g after 500 cycles at 0.5 A/g	89.8%, 0.02%	4
MC-CNF/MoSe2	386 mAh/g after 300 cycles at 0.5 A/g	90.3%, 0.032%	5
MoSe2@C@G	367 mAh/g after 200 cycles at 0.2 A/g	86.2%, 0.069%	6
MoSe2@C/N,P-rGO	337 mAh/g after 100 cycles at 0.5 A/g	90.3%, 0.097%	7
MoSe2/C	404 mAh/g after 100 cycles at 0.2 A/g	82.9%, 0.171%	8
MoSe2/rGO	247 mAh/g after 100 cycles at 0.1 A/g	82.3%, 0.177%	9
MoSe2/CNT	296 mAh/g after 50 cycles at 1.0 A/g	83%, 0.34%	10
MoSe2/G	358 mAh/g after 50 cycles at 0.4 A/g	95%, 0.1%	11
MoSe2 nanoplates	369 mAh/g after 50 cycles at 0.1 A/g	71.9%, 0.562%	12
1D-MoSe2@C	415 mAh/g after 30 cycles at 0.2 A/g	96.3%, 12.3%	13

Table S3. The performance of optimized sample in this work in comparision with the previously reported $MoSe_2$ composites for PIBs.

Anode	Performance	Retention, Attenuation Per cycle	Ref.
MoSe2-MoO3/C	302 mAh/g after 300 cycles at 0.05 A/g	97.9%, 0.007%	This work
MoSe2/N-C	258 mAh/g after 300 cycles at 0.1 A/g	92.7%, 0.024%	14
MoSe2/P, N-C	260 mAh/g after 200 cycles at 0.1 A/g	93.9%, 0.030%	15
MoSe2/C	322 mAh/g after 100 cycles at 0.2 A/g	83.9%, 0.161%	16
HM-MoSe2/N-C	223 mAh/g after 100 cycles at 0.1 A/g	85.1%, 0.149%	17
MoSe2/C fibers	316 mAh/g after 100 cycles at 0.1 A/g	63.2%, 0.368%	18
$MoSe_2$@N-CNT	247 mAh/g after 100 cycles at 0.1 A/g	56.1%, 0.439%	19
N-MoSe2/G	330 mAh/g after 30 cycles at 0.2 A/g	82.1%, 0.597%	20

References.

1. F. Niu, J. Yang, N. Wang, D. Zhang, W. Fan, J. Yang and Y. Qian, *Adv. Funct. Mater.*, 2017, **27**, 1700522.
2. F. Zheng, W. Zhong, Q. Deng, Q. Pan, X. Ou, Y. Liu, X. Xiong, C. Yang, Y. Chen and M. Liu, *Chem. Eng. J.*, 2019, **357**, 226-236.
3. M. Yousaf, Y. Wang, Y. Chen, Z. Wang, A. Firdous, Z. Ali, N. Mahmood, R. Zou, S. Guo and R. P. S. Han, *Adv. Energy Mater.*, 2019, **9**, 1900567.
4. G. Jia, H. Wang, D. Chao, H. He, N. H. Tiep, Y. Zhang, Z. Zhang and H. J. Fan, *Nanotechnology*, 2017, **28**, 42LT01.
5. S. Young Jeong, S. Ghosh, J.-K. Kim, D.-W. Kang, S. Mun Jeong, Y. Chan Kang and J. S. Cho, *Journal of Industrial and Engineering Chemistry*, 2019, **75**, 100-107.
6. C. Cui, G. Zhou, W. Wei, L. Chen, C. Li and J. Yue, *J. Alloy Compd.*, 2017, **727**, 1280-1287.

7. L. B. Tang, B. Zhang, C. S. An, H. Li, B. Xiao, J. H. Li, Z. J. He and J. C. Zheng, *Inorganic chemistry*, 2019, **58**, 8169-8178.

8. Q. Su, X. Cao, X. Kong, Y. Wang, C. Peng, J. Chen, B. Yin, J. Shi, S. Liang and A. Pan, *Electrochim. Acta.*, 2018, **292**, 339-346.

9. B.-M. Zhang, C.-B. Zhang, H. Zhang, Y.-X. Hu, Y.-S. Zhang, C. Lu, J. Li, L.-B. Kong and M.-C. Liu, *Applied Surface Science*, 2020, **513**, 145826.

10. S. H. C. a. Y. C. Kang*, *Nanoscale*, 2016, **8**, 4209-4216.

11. X. Zhao, W. Cai, Y. Yang, X. Song, Z. Neale, H.-E. Wang, J. Sui and G. Cao, *Nano Energy*, 2018, **47**, 224-234.

12. H. Wang, X. Lan, D. Jiang, Y. Zhang, H. Zhong, Z. Zhang and Y. Jiang, *J. Power Sources*, 2015, **283**, 187-194.

13. S. Tian, *Ceram Int*, 2019, **45**, 21423-21429.

14. J. Ge, L. Fan, J. Wang, Q. Zhang, Z. Liu, E. Zhang, Q. Liu, X. Yu and B. Lu, *Adv. Energy Mater.*, 2018, **8**, 1801477.

15. B. Li, Y. Liu, Y. Li, S. Jiao, S. Zeng, L. Shi and G. Zhang, *ACS Appl. Mater. Interfaces*, 2020, **12**, 2390-2399.

16. W. Wang, B. Jiang, C. Qian, F. Lv, J. Feng, J. Zhou, K. Wang, C. Yang, Y. Yang and S. Guo, *Adv. Mater.*, 2018, **30**, e1801812.

17. Y. Liu, Y. Zhai, N. Wang, Y. Zhang, Z. Lu, P. Xue, L. Bai, M. Guo, D. Huang and Z. Bai, *ChemistrySelect*, 2020, **5**, 2412-2418.

18. Q. Shen, P. Jiang, H. He, C. Chen, Y. Liu and M. Zhang, *Nanoscale*, 2019, **11**, 13511-13520.

19. N. Li, L. Sun, K. Wang, J. Zhang and X. Liu, *Electrochim. Acta*, 2020, **360**, 136983.

20. Y. Yi, Z. Sun, C. Li, Z. Tian, C. Lu, Y. Shao, J. Li, J. Sun and Z. Liu, *Adv. Funct. Mater.*, 2020, **30**, 1903878.